Research paper

Synthesis, Crystal Structures, and Superoxide Dismutase Activity of Two New Multinuclear Manganese(III)-Salen-4,4'-Bipyridine Complexes

Yusi Deawati, Djulia Onggo, Irma Mulyani, Iwan Hastiawan, Dikdik Kurnia, Peter Lönnecke, Sara Schmorl, Berthold Kersting, Evamarie Hey-Hawkins

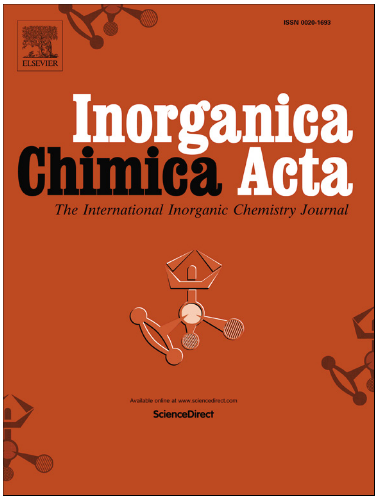

PII: S0020-1693(18)30324-4
DOI: https://doi.org/10.1016/j.ica.2018.06.018
Reference: ICA 18310

To appear in: *Inorganica Chimica Acta*

Received Date: 1 March 2018
Revised Date: 9 June 2018
Accepted Date: 11 June 2018

Please cite this article as: Y. Deawati, D. Onggo, I. Mulyani, I. Hastiawan, D. Kurnia, P. Lönnecke, S. Schmorl, B. Kersting, E. Hey-Hawkins, Synthesis, Crystal Structures, and Superoxide Dismutase Activity of Two New Multinuclear Manganese(III)-Salen-4,4'-Bipyridine Complexes, *Inorganica Chimica Acta* (2018), doi: https://doi.org/10.1016/j.ica.2018.06.018

Research Paper

Synthesis, Crystal Structures, and Superoxide Dismutase Activity of Two New Multinuclear Manganese(III)-Salen-4,4’-Bipyridine Complexes

Yusi Deawati*[1], Djulia Onggo[1], Irma Mulyani[1], Iwan Hastiawan[2], Dikdik Kurnia[3], Peter Lönnecke[4], Sara Schmorl[4], Berthold Kersting[4], Evamarie Hey-Hawkins[4]

[1]Inorganic and Physical Chemistry Research Group, Faculty of Mathematics and Natural Sciences, Institut Teknologi Bandung, Indonesia
[2]Physical and Inorganic Chemistry Laboratory, Faculty of Mathematics and Natural Sciences, Universitas Padjadjaran, Indonesia
[3]Organic Chemistry Laboratory, Faculty of Mathematics and Natural Sciences, Universitas Padjadjaran, Indonesia
[4]Institut für Anorganische Chemie, Fakultät für Chemie und Mineralogie, Universität Leipzig, Germany

*Corresponding author.
E-mail address: yusi.deawati@unpad.ac.id
Full postal address: Program Studi Doktor Kimia, Gedung Kimia Baru, FMIPA, Institut Teknologi Bandung,
Jl. Ganesha No. 10, Bandung, Indonesia, 40132, phone no. +6222 2502103

Manganese(III)-salen complexes have been reported as superoxide dismutase mimics (mSOD) that can scavenge superoxide anion radicals. They are mononuclear complexes with a variety of salen ligands. Here, two new multinuclear manganese(III)-salen complexes with 4,4’-bipyridine (4,4’-bpy) as bridging ligand and ClO_4^- as axial ligand or PF_6^- as counter anion, respectively, are reported. The dimeric complex $[\{Mn(ClO_4)(salen)\}_2(\mu\text{-}4,4'\text{-bpy})]$ (**1**) was obtained from $[MnCl(salen)]\cdot 2H_2O$ and 4,4’-bipyridine which followed by addition of $NaClO_4$. While the polymeric complex $\{[Mn(salen)(4,4'\text{-bpy})]PF_6\}_n$ (**2**) was prepared by the same procedure of **1**, followed by addition of KPF_6 replacing $NaClO_4$. Compounds **1** and **2** were characterized by elemental analysis, conductometry, infrared spectroscopy, electrospray-ionization mass spectrometry, and room temperature/variable temperature magnetic susceptibility measurements. The crystal structures of compounds **1** and **2** were determined by single crystal X-ray crystallography. Furthermore, in indirect SOD tests using riboflavin photoreduction, the polymeric compound **2** shows the slightly higher SOD activity with an IC_{50} of 1.6 ± 0.2 μM than the dimeric compounds **1** with an IC_{50} of 2.0 ± 0.3 μM.

Keywords: manganese-salen-4,4’-bipyridine, dimeric, polymeric, superoxide dismutase, SOD, mimic, riboflavin, photoreduction

Introduction

Superoxide radical is a highly dangerous reactive oxygen species [1]. It may cause damage to human tissues that are often associated with various diseases, such as rheumatoid arthritis, cancer, neurodegenerative disorder, diabetic complication, stroke, inflammation, and reperfusion injuries [2, 3].

Normally, the enzyme superoxide dismutase (SOD) acts as a catalyst in the conversion of superoxide radicals to hydrogen peroxide and oxygen [4, 5]. However, if large amounts of superoxide radicals are present, the amount of SOD will not be adequate; therefore, uptake of an exogenous SOD is required. It was observed that the use of natural SOD was not effective, caused immunogenicity and was also rather expensive, while the use of SOD mimics instead showed many advantages [3, 6].

Several manganese(III)-salen complexes (salen = N,N’-bis(salicylidene)-1,2-ethylenediamine) have been reported as SOD mimics with low toxicity [7]. They were obtained as mononuclear complexes with a variety of salen ligands. Several monomeric manganese(III)-salen complexes had been modified through substitution of their salen ring, such as [Mn(OMe-salen)(OAc)], [Mn(OEt-salen)(OAc)], [Mn(OMe-salen)Cl], [Mn(OEt-salen)Cl], were showed similar activity of SOD mimic to the normal (unsubstituted) one, i.e. [Mn(salen)OAc] and

[Mn(salen)Cl] [8, 9]. [Mn(salen)OAc] was included in the first compounds that have activity as SOD mimics. Its SOD mimic activity is expressed by IC_{50} of 2.7 ± 0.1 μM through non-enzymatic indirect method of photoreduction riboflavin-nitrobluetetrazolium SOD assay [10]. So far, no multinuclear manganese(III)-salen reported as SOD mimics.

Bridging ligands such as 4,4'-bipyridine (4,4'-bpy) facilitate the formation of dimeric or polymeric manganese(III)-salen complexes. However, in $[Mn(salpn)(CH_3OH)(4,4'\text{-bpy})]BPh_4$ (salpn = N,N'-bis(salicylidene)-1,3-diaminopropane) [11], 4,4'-bpy does not act as a bridging ligand, and a mononuclear complex was obtained. With 3,3'-bpy, the polymeric complex $[Mn(salen)(3,3'\text{-bpy})]Tf_2N$ (Tf_2N = bis(trifluoro methanesulfonyl)amide) was obtained [12].

The presence of counter anions also contributes to the structural aspects of manganese(III)-salen complexes. With chloride or acetate anions, usually mononuclear complexes were obtained. However, when perchlorate (ClO_4^-) and hexafluorophosphate (PF_6^-) anions are involved, dimeric complexes were formed [13-16].

Here, we report the synthesis and characterization of manganese(III)-salen multinuclear complexes containing 4,4'-bpy bridging ligand and ClO_4^- axial ligand or PF_6^- counter anion. This study is neded to investigate the effect of multinuclear structural to SOD activity. The SOD activity of the two resulting complexes was studied.

Experimental

Materials and Methods

Chemicals including solvents used without further purification in the preparation and characterization of manganese(III)-salen complexes have been purchased from Sigma-Aldrich. Elemental analyses (C, H, N) were carried out using a Vario EL III from elemental analyzer system GmbH. Conductivities of 10^{-3} M solutions in methanol were measured on a HANNA Instruments HI 8819W Professional ATC conductivity meter. Infrared spectra (400 - 4000 cm^{-1}) were recorded as KBr pellets on a PerkinElmer System 2000 FTIR spectrometer. Electrospray ionization mass spectra (ESI-MS) were obtained on a Bruker Daltonics ESQUIRE 3000Plus (ESI-Ion Trap MSn) spectrometer. Magnetic susceptibilities at room-temperature were measured using a Magnetic Susceptibility Balance (MSB) from Sherwood Scientific. Temperature-dependent magnetic susceptibility measurements on powders were carried out using an MPMS 7XL SQUID magnetometer (Quantum Design) over the temperature range 2–330 K at an applied magnetic field of 1.0 Tesla.

Synthesis

H_2salen

The ligand H_2salen was prepared salicylaldehyde and ethylenediamine in ethanol following the published procedure [17]. A yellow solid was formed during the reaction (yield 80-88%). Anal. calc. for $C_{16}H_{16}N_2O_2$ (268.31): C, 71.62; H, 6.01; N, 10.44; found: C, 71.60; H, 6.05; N, 10.44 %. Conductivity (in methanol) $\Lambda_M = 0$ μS. IR (KBr, cm^{-1}): ν(O-H) 3425 (m), ν(C=N) 1636 (vs), ν(C-O) 1283 (s). ESI [MS]: *m/z* 269 $[H_2salen+H]^+$.

$[MnCl(salen)]\cdot 2H_2O$

The compound was prepared from manganese(II) chloride tetrahydrate and H_2salen in ethanol according to the published procedure [18]. Upon standing at room temperature for 3 days, brown-black crystals formed. These were isolated by filtration, washed with water and ethanol, and dried in the air. Yield 75-90%. Anal. calc. for $C_{16}H_{14}ClMnN_2O_2$ (392.72): C, 48.93; H, 4.62; N, 7.13; found: C, 48.36; H, 4.34; N, 7.13 %. Conductivity (in methanol) $\Lambda_M = 0.17$ mS. IR (KBr, cm^{-1}): ν(O-H) 3426 (m), ν(C=N) 1634 (vs), ν(C-O) 1292 (s). ESI [MS]: *m/z* 321.9 $[Mn(salen)]^+$. Magnetic moment: $\mu_{eff} = 5.22\ \mu_B$.

$[\{Mn(salen)(ClO_4)\}_2(\mu\text{-}4,4'\text{-bpy})]$ (1)

The complex was prepared from $[MnCl(salen)]\cdot 2H_2O$ (0.39 g, 1 mmol) in methanol (20 mL) and 4,4'-bipyridine (0.31 g, 2 mmol) in methanol (20 mL) at 50 °C. During the reaction, an aqueous solution of $NaClO_4$ (1 g in 5 mL) was added and then the solvent was reduced slowly. After cooling to room temperature, the solution was filtered to remove any unwanted precipitate. Upon standing at room temperature for 3 days, brown-black crystals were formed. These were isolated by filtration, washed with methanol, and dried in air. Yield 70-88%. Anal. calc. for $C_{42}H_{36}Cl_2Mn_2N_6O_{12}$ (997.55): C, 50.57; H, 3.64; N, 8.42; found: C, 50.23; H, 3.25; N, 8.45 %. Conductivity (in methanol) $\Lambda_M = 0.24$ mS. IR (KBr, cm^{-1}): ν(O-H) 3417 (m), ν(C=N) 1621 (vs), ν(C-O) 1287 (s). ESI [MS]: *m/z* 677.0 $[Mn(salen)(4,4'\text{-bpy})_2+CH_3CN]^+$; 743.0 $[Mn_2(salen)_2(ClO_4)+H]^+$. Magnetic moment: $\mu_{eff} = 6.86\ \mu_B$.

{[Mn(salen)(μ-4,4'-bpy)]PF_6}$_n$·1.5MeOH·0.5H_2O (2)

A similar procedure as stated above for **1** was used to prepare this complex, using KPF_6 (1 g in 15 mL) instead of $NaClO_4$. Deep brown crystals were obtained; yield 65-85%. Anal. calc. for $C_{27.5}H_{29}F_6MnN_4O_4P$ (679.46): C, 48.76; H, 3.78; N, 8.75; found: C, 48.21; H, 3.62; N, 8.69 %. Conductivity (in methanol) Λ_M = 0.27 mS. IR (KBr, cm^{-1}): ν(O-H) 3453 (m), ν(C=N) 1602 (vs), ν(C-O) 1289 (s). ESI [MS]: *m/z* 661 [Mn(salen)(4,4'-bpy)(PF_6)·1.5MeOH·0.5H_2O + H]$^+$. Magnetic moment: μ_{eff} = 4.8 μ_B.

SOD-Mimic Activity Assay

The SOD-mimic activity of complexes **1** and **2** were evaluated using an indirect method of riboflavin photoreduction, which was described previously [10, 19]. The method involves the competitive reaction between the complex and reduced NBT (NBT = nitroblue tetrazolium) for $O_2^{\bullet-}$ generated by riboflavin under illumination at room temperature (25 °C). The sample mixture (240 μL) contained the complex (11 different concentrations), 6 μM riboflavin (Thermo Scientific), 0.8 μM of N,N,N',N'-tetramethylethylene-diamine (TMEDA) (Biorad) in 0.016 M phosphate buffer (pH 7.4) and 85 μM NBT (Thermo Scientific). The reaction was stopped by switching off the light after 15 min (4 fluorescence tubes, Philips TLD/20 W, 20 cm distance) and the absorbance of reduced NBT was measured at λ 560 nm with a Multiskan Go Thermo Fischer Scientific UV/Vis double beam spectrophotometer.

Crystal Data Collection and Refinement

The single crystal of **1** and **2** were obtained from methanol. Single crystal X-ray data were collected on a Gemini CCD diffractometer (Rigaku, Inc.) with graphite-monochromated Mo-Kα radiation (λ = 0.71073 Å) and ω-scan rotation in the θ range 2.412 to 30.414° (**1**) and 1.884 to 32.400° (**2**) at 130 K. Information regarding the crystallographic data collection and refinement parameters of the structures are compiled in Table 1 and Table 3, respectively. Semi-empirical absorption correction from equivalents was applied to the data. The structures were solved with SHELXT-2014 [20]. Disorderd solvent molecules and a minor disordered fraction of the PF_6^- anion in **2** were refined isotropically, whereas all other non-hydrogen atoms were refined anisotropically by full-matrix least-squares techniques on F^2 with SHELXL-2016 [21]. Except disordered moieties, all hydrogen atoms were located on difference Fourier maps calculated at the final stage of the structure refinement. The isotropic displacement parameter for H(17) and H(18) of compound **1** are fixed. The three methanol and one water molecule are highly disordered for symmetry reasons. The electron density of all solvent molecules has been confirmed with the SQUEEZE routine implemented in PLATON. The SQUEEZE electron count revealed 63 electrons for all disordered solvent molecules, which is in excellent agreement with the above given composition (3 MeOH + 1 H_2O = 64 electrons). Solvent hydrogen donor-acceptor bonds (Table 5) are illustrated in Figure 4(b). The position of oxygen bonded hydrogen atoms was deduced from adjacent hydrogen acceptor atoms. Figures of crystal structures were drawn using the program Diamond-3 [22]. Selected bond lengths and angles for complexes **1** and **2** are listed in Tables 2 and 4.

CCDC 1579051 (**1**) and 1579052 (**2**) contain the supplementary crystallographic data for this paper. These data can be obtained free of charge via https://summary.ccdc.cam.ac.uk/structure-summary-form (or from the Cambridge Crystallographic Data Centre, 12 Union Road, Cambridge CB2 1EZ, UK; fax: (+44)1223-336-033; or deposit@ccdc.cam.ac.uk).

Results and Discussion

Synthesis

Compounds **1** and **2** were prepared from reaction between [MnCl(salen)]·2H_2O and 4,4'-bpy to give deep brown solution, with further addition of a saturated $NaClO_4$ or KPF_6 solution, respectively. The crystal of compounds **1** and **2** have the similar deep brown colours, but **1** forms longer crystal than **2**. The structures of both complexes were obtained by single crystal XRD.

Crystal Structures

[{Mn(salen)(ClO_4)}$_2$(μ-4,4'-bipyridine)] (1)

Compound **1** crystallized in the triclinic space group $P\bar{1}$ (Table 1). It is a neutral centrosymmetric manganese(III) complex coordinated by salen, bipyridine and the perchlorate anion in a distorted octahedral fashion caused by the Jahn-Teller effect (Figure 1).

The four donor atoms of the tetradentate salen ligand, a Schiff base, occupy the equatorial plane [Mn-O

1.874(2) and 1.876(2) Å, and Mn-N 1.978(2) and 1.968(2) Å], while the axial bond lengths to an N donor atom in 4,4’-bpy [2.296(2) Å] and an O atom of perchlorate [2.433(2) Å] are longer (Table 2).

Table 1. Crystallographic data of [{Mn(salen)(ClO_4)}$_2$(μ-4,4’-bpy)] (**1**).

Empirical formula	$C_{42}H_{36}Cl_2Mn_2N_6O_{12}$
Formula weight	997.55
T / K	130(2)
Wavelength / Å	0.71073
Crystal system	Triclinic
Space group	$P\bar{1}$
Unit cell dimensions:	
a / Å	8.3114(4)
b / Å	8.6461(5)
c / Å	14.7044(9)
α / °	77.959(5)
β / °	79.477(5)
γ / °	85.071(5)
V / $Å^3$	1014.8(1)
Z	1
ρ_{calcd} / Mg m^{-3}	1.632
Absorption coefficient / mm^{-1}	0.829
F(000)	510
Crystal size / mm^3	0.3 x 0.15 x 0.02
θ range for data collection / °	2.412 to 30.414
Reflections collected	10286
Independent reflections / R_{int}	5493 (0.0482)
Completeness to θ = 28.285° / %	99.9
Max. and min. transmission	1 and 0.75023
Data / restraints / parameters	5493 / 0 / 359
Goodness-of-fit on F^2	0.997
Final R indices [I>2σ(I)]	R1 = 0.0543, wR2 = 0.0996
R indices (all data)	R1 = 0.1043, wR2 = 0.1206
Largest difference in peak and hole /e·$Å^{-3}$	0.584 and -0.880

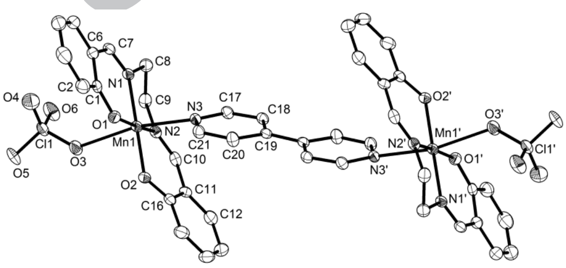

Figure 1. ORTEP view of [{Mn(salen)(ClO_4)}$_2$(μ-4,4’-bpy)] (**1**).

Table 2. Selected bond lengths (Å) and angles (°) in [{Mn(salen)(ClO_4)}$_2$(μ-4,4’-bpy)] (**1**).

Mn(1)-O(1)	1.874(2)
Mn(1)-O(2)	1.876(2)
Mn(1)-N(2)	1.968(2)
Mn(1)-N(1)	1.978(2)
Mn(1)-N(3)	2.296(2)
Mn(1)-O(3)	2.433(2)

O(1)-Mn(1)-O(2)	94.13(9)	N(2)-Mn(1)-N(3)	94.20(9)
O(1)-Mn(1)-N(2)	172.64(9)	N(1)-Mn(1)-N(3)	98.85(9)
O(2)-Mn(1)-N(2)	91.91(9)	O(1)-Mn(1)-O(3)	88.96(8)
O(1)-Mn(1)-N(1)	92.0(1)	O(2)-Mn(1)-O(3)	83.85(8)
O(2)-Mn(1)-N(1)	173.1(1)	N(2)-Mn(1)-O(3)	87.51(9)
N(2)-Mn(1)-N(1)	81.7(1)	N(1)-Mn(1)-O(3)	93.21(9)
O(1)-Mn()-N(3)	90.60(9)	N(3)-Mn(1)-O(3)	167.93(8)
O(2)-Mn(1)-N(3)	84.16(8)		

{[Mn(salen)(μ-4,4’-bipyridine)]PF_6}$_n$·1.5MeOH·0.5H_2O (2)

Compound **2** is ionic and crystallizes in the triclinic space group $P\bar{1}$ (Table 3) with one [Mn(salen)(4,4'-bpy)]$^+$ cation and one PF_6^- anion in the asymmetric unit (Figure 4(a)). As illustrated in Figure 4(b), the manganese(III)-salen units are interconnected by bridging 4,4’-bpy ligands forming polymeric cationic chains along (010). Disordered co-crystallized solvent molecules (3MeOH and H_2O) were located near a center of inversion (Figure 4(c)) and could be identified with the help of significant hydrogen donor-acceptor bonds (Table 5). As expected, the manganese(III) ion adopts a six-coordinated distorted octahedral coordination geometry (Table 4). The two pyridyl rings in 4,4'-bpy are rotated with respect to each other. The angle between the planes of the two crystallographically different pyridyl rings in 4,4'-bipyridine is 52.18(8)°. The four donor atoms of the salen occupied the equatorial plane [Mn-O 1.870(2) and 1.871(2) Å, and Mn-N 1.972(2) and 1.973(2) Å].

Table 3. Crystallographic data of $\{[Mn(salen)(\mu\text{-}4,4'\text{-}bpy)]PF_6\}_n\cdot 1.5MeOH\cdot 0.5H_2O$ (**2**).

Empirical formula	$C_{27.5}H_{29}F_6MnN_4O_4P$
Formula weight	679.46
T / K	130(2)
Wavelength / Å	0.71073
Crystal system	Triclinic
Space group	$P\overline{1}$
Unit cell dimensions:	
a / Å	8.9522(6)
b / Å	11.7888(4)
c / Å	15.4129(7)
α / °	105.939(3)
β / °	105.231(5)
γ / °	101.932(4)
V / $Å^3$	1439.3(1)
Z	2
ρ_{calcd} / Mg m^{-3}	1.568
Absorption coefficient / mm^{-1}	0.595
F(000)	696
Crystal size / mm^3	0.25 x 0.25 x 0.15
θ range for data collection / °	1.884 to 32.400
Reflections collected	16890
Independent reflections / R_{int}	9371 (0.0341)
Completeness to θ = 28.285° / %	100.0
Max. and min. transmission	1 and 0.97458
Data / restraints / parameters	9371 / 24 / 508
Goodness-of-fit on F^2	1.019
Final R indices [I>2σ(I)]	R1 = 0.0591, wR2 = 0.1324
R indices (all data)	R1 = 0.0937, wR2 = 0.1524
Largest difference in peak and hole / e·$Å^{-3}$	0.860 and -0.700

Table 4. Selected bond lengths (Å) and angles (°) in $[Mn(salen)(\mu\text{-}4,4'\text{-}bpy)]PF_6\cdot 1.5MeOH \cdot 0.5H_2O$ (**2**)

Mn(1)-O(1)	1.870(2)		
Mn(1)-O(2)	1.871(2)		
Mn(1)-N(2)	1.973(2)		
Mn(1)-N(1)	1.972(2)		
Mn(1)-N(3)	2.368(2)		
Mn(1)-N(4)	2.372(2)		
O(1)-Mn(1)-O(2)	93.03(7)	N(2)-Mn(1)-N(3)	87.00(8)
O(1)-Mn(1)-N(2)	174.59(8)	N(1)-Mn(1)-N(3)	89.92(7)
O(2)-Mn(1)-N(2)	92.29(8)	O(1)-Mn(1)-N(4)	89.57(7)
O(1)-Mn(1)-N(1)	92.21(8)	O(2)-Mn(1)-N(4)	91.11(7)
O(2)-Mn(1)-N(1)	174.54(8)	N(1)-Mn(1)-N(4)	87.38(7)
N(2)-Mn(1)-N(1)	82.50(8)	N(2)-Mn(1)-N(4)	91.32(7)
O(1)-Mn(1)-N(3)	91.87(7)	N(3)-Mn(1)-N(4)	176.99(7)
O(2)-Mn(1)-N(3)	91.45(7)		

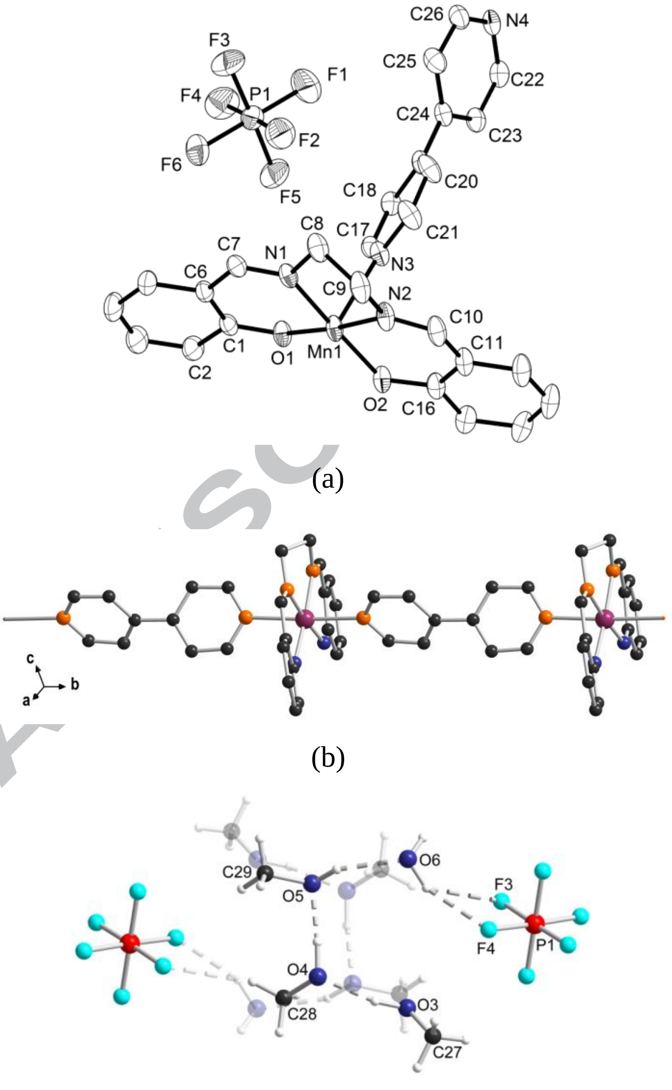

(a)

(b)

(c)

Figure 4. (a) ORTEP view of the asymmetric unit of $\{[Mn(salen)(\mu\text{-}4,4'\text{-}bpy)]PF_6\}_n\cdot 1.5MeOH\cdot 0.5H_2O$ (**2**) (H atoms and solvent molecules are omitted); (b) coordination polymer along (010); (c) solvent molecules located on (00½). The disordered fraction is transparent for clarity.

Table 5. Hydrogen bond distances (Å) and angles (°) in $\{[Mn(salen)(\mu\text{-}4,4'\text{-}bpy)]PF_6\}_n\cdot 1.5MeOH \cdot 0.5H_2O$ (**2**).

D-H···A	d(D-H)	d(H···A)	d(D···A)	<(DHA)
O(3)-H(1O3) ···O(4)	0.98	1.72	2.650(1)	156.6
O(4)-H(1O4) ···O(5)	0.98	1.69	2.658(9)	171.8
O(5)-H(1O5) ···O(6)	0.98	2.03	2.914(9)	148.8

Symmetry transformations used to generate equivalent atoms:
#1 x,y+1,z #2 x,y-1,z

Magnetic Properties

The magnetic properties of compound **1** were investigated by temperature-dependent magnetic susceptibility measurements in the temperature range between 2 and 330 K and an external field of $B = \mu_0 H$ = 1.0 T. Figure 5 shows the experimental data and the theoretical fit in the form of a μ_{eff} versus T plot. At 330 K, μ_{eff} is 6.92 μ_{B}, which is in good agreement with the presence of two high-spin Mn$^{\mathrm{III}}$ ions (S = 2). With decreasing temperature, the effective magnetic moment remains nearly constant down to 20 K. For lower temperatures, it decreases faster to a value of μ_{eff} = 5.39 μ_{B} at 2 K. This curve progression shows a weak antiferromagnetic exchange interaction between the two manganese(III) atoms. This is further corroborated by the continuous decrease of the μ_{eff} values from 6.93 μ_{B} at 330 K to 5.39 μ_{B} at 2 K.

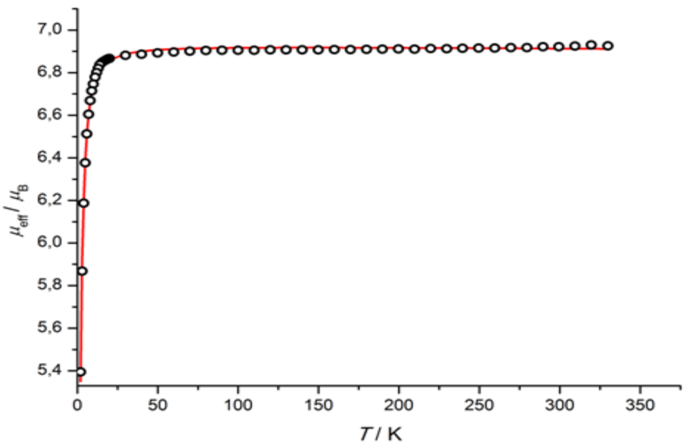

Figure 5. Temperature dependence of μ_{eff} for [{Mn(salen)(ClO$_4$)}$_2$(μ-4,4’-bpy)] (**1**) per dinuclear unit. The solid line represents the best theoretical fit to the spin Hamiltonian (eq. 1).

The temperature dependence of the magnetic susceptibility was simulated using the appropriate spin Hamiltonian (eq. 1), which includes the isotropic Heisenberg-Dirac-vanVleck exchange(HDvV), the single-ion zero-field splitting and the single-ion Zeeman interaction by using a full-matrix diagonalization approach.

$$\hat{H} = (-2J\hat{S}_1\hat{S}_2) + \mu_B \sum_{i=2}^{2} (g\hat{S}_i\hat{B}) + \sum_{i=2}^{2} D_i \left(\hat{S}_{zi}^2 - \frac{1}{3}(S_i(S_i+1))\right) \quad \text{eq. 1}$$

Scheme 1 illustrates the exchange coupling pathways used to model the susceptibility data for complex **1**. In this model, the exchange interaction between the neighboring Mn$^{\mathrm{III}}$ ions are represented by $J_{1/2}$. The g values were considered to be identical for the two Mn$^{\mathrm{III}}$ ions. A reasonable fit of the experimental susceptibility data was possible over the full range and led to $J_{1/2}$ = -0.042 cm^{-1}, D = 2.38 cm^{-1} and g = 2.0.

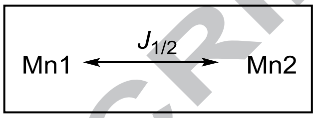

Scheme 1. Magnetic exchange pathways used for simulation of the magnetic susceptibility data for the dinuclear subunits in [{Mn(salen)(ClO$_4$)}$_2$(μ-4,4’-bpy)] (**1**).[a]

Table 6. Magnetic properties of [{Mn(salen)(ClO$_4$)}$_2$(μ-4,4’-bpy)] (**1**).

Complex	g	J [cm^{-1}]	D [cm^{-1}]	TIP [cm^{3}mol^{-1}]
2	2.0	$J_{1/2}$ = -0.042	2.38	8.80 x 10^{-5}

[a] Parameters resulting from least-squares fit to be μ_{eff} data under the spin Hamiltonian in eq. 1: J = coupling constant ($H = -2JS_1S_2$), g = g value, D = zero-field splitting parameter and TIP = temperature-independent paramagnetism.

SOD-mimic Activity

The mSOD activities of the three manganese(III)-salen complexes **1**, and **2** were evaluated quantitatively using the indirect method of riboflavin photoreduction in the presence of TMEDA. Riboflavin was reduced photochemically in air generating superoxide anions, which in turn reduced NBT. The results of this assay indicated that approximately 2.0 ± 0.3 µM of compound **1** or 1.6 ± 0.2 µM of compound **2** was needed in order to inhibit 50% of the NBT photoreduction (termed as IC$_{50}$). The degree of inhibition is increased in a concentration-dependent manner for the three compounds that allowed plotting IC$_{50}$ values (Table 7 and Figure 6).

Table 7. The inhibition percentage of complexes **1** and **2** from the mSOD assay.

No.	Concentration (μM)	Inhibition (%)	
		Complex 1	Complex 2
1	0	0	0
2	1	27	43
3	2	50	57
4	3	62	70
5	4	74	75
6	6	83	84
7	10	89	93
8	20	95	97

These IC_{50} values are in the range of the IC_{50} of mSOD [6], which means that the superoxide anion radical scavenging effects of the two manganese(III)-salen complexes **1**, and **2** were effectively inhibiting NBT reduction.

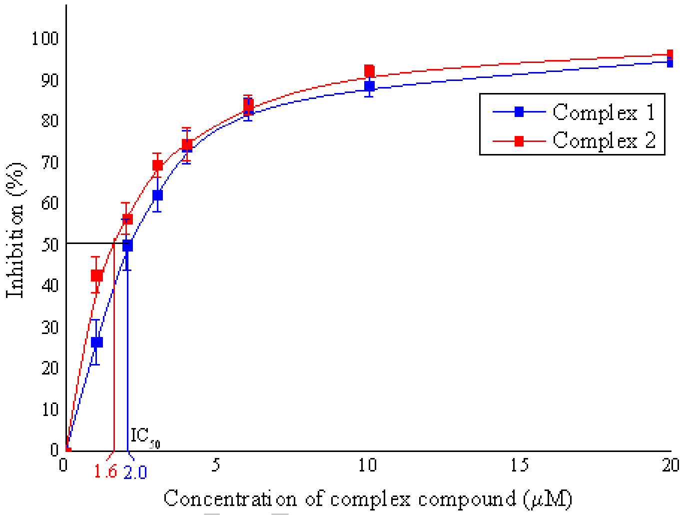

Figure 6. The mSOD activity curves of complexes **1** and **2**, and the IC_{50} values.

The polymeric compound **2** shows the higher SOD activity than the dimeric compound **1**. The different IC_{50} values obtained from the riboflavin photoreduction mSOD assay clearly indicate that structural differences of the two complexes affect SOD activity. It seems that the polymeric structure is better at facilitating the redox cycle of the Mn^{III}-Mn^{II} ions in the superoxide dismutation than the dimeric structure and through the same method, both of the multinuclear complexes have better ativities than the mononuclear [Mn(salen)OAc] complex.

Conclusions

Two new multinuclear manganese(III)-salen complexes containing 4,4'-bipyridine bridging ligand and ClO_4^- axial ligand or PF_6^- counter anion, namely dimeric $[\{Mn(salen)(ClO_4)\}_2(\mu\text{-}4,4'\text{-bpy})]$ (**1**), and polymeric $\{[Mn(salen)(\mu\text{-}4,4'\text{-bpy})]PF_6\}_n$ (**2**), were prepared and structurally characterized. Their SOD mimic activity was determined and indicates that structural features affect SOD activity.

Acknowledgments

This study was supported by a scholarship of BPPDN 2013, a scholarship of Sandwich-like Program (PKPI) 2015, and Doctoral Grants 2017 (No. 006/ADD/SP2H/LT/DRPM/VIII/2017 from the Directorate Generale of Higher Education, Republic of Indonesia. We would like to thank Dr. Debbie S. Retnoningrum from the Pharmaceutical Biotechnology Laboratory, School of Pharmacy, Institut Teknologi Bandung, for support with the SOD-*like* assays.

References

[1] J. M. McCord and I. Fridovich, "Enzymology: The Reduction of Cytochrome c by Milk Xanthine Oxidase," *The Journal of Biological Chemistry*, vol. 243, pp. 5753-5760, 1968.

[2] J. M. McCord and I. Fridovich, "Superoxide Dismutase. an Enzymic Function for Erythrocuprein (Hemocuprein)," *The Journal of Biological Chemistry*, pp. 244, 6049 – 6055, 1969.

[3] F. Johnson and C. Giulivi, "Superoxide Dismutases and their Impact Upon Human Health," *Molecular Aspects of Medicine*, vol. 26, pp. 340-352, 2005.

[4] J. M. McCord and M. A. Edeas, "SOD, Oxidative Stress and Human Pathologies: a Brief History and a Future Vision," *Biomedicine and Pharmacotherapy*, vol. 59, p. 139–142, 2005.

[5] K. Pong, "Oxidative Stress in Neurodegenerative Diseases: Therapeutic Implications for Superoxide Dismutase Mimetics. Expert Opinion on Biological Therapy," *Expert Opinion on Biological Therapy, Informa Healthcare*, vol. 3, p. 127–139, 2003.

[6] O. Iranzo, "Minireview. Manganese Complexes Displaying Superoxide Dismutase Activity: A Balance Between Different Factors," *Bioorganic Chemistry,* vol. 39, pp. 73-87, 2011.

[7] P. D. Riley, "Functional Mimics of Superoxide Dismutase Enzymes as Therapeutic Agents," *Chemical Reviews,* vol. 99, pp. 2573-2588, 1999.

[8] M. Baudry, S. Etienne, A. Bruce, M. Palucki, E. Jacobsen and B. Malfroy, "Salen-Manganese Complexes are Superoxide Dismutase-Mimics," *Biochemical and Biophysical Research Communications,* vol. 192, pp. 964-968, 1993.

[9] S. Doctrow, K. Huffman, C. B. Marcus, G. Tocco, E. Malfroy, C. A. Adinolfi, H. Kruk, K. Baker, N. Lazarowych, J. Mascarenhas and B. Malfroy, "Salen-Manganese Complexes as Catalytic Scavengers of Hydrogen Peroxide and Cytoprotective Agents: Structure-Activity Relationship Studies," *Journal of Medicinal Chemistry,* vol. 45, pp. 4549-4558, 2002.

[10] Y. Deawati, D. Onggo, I. Mulyani, I. Hastiawan and D. Kurnia, "Activity of Superoxide Dismutase Mimic of [Mn(salen)OAc] Complex Compound Non-enzymatically In Vitro through Riboflavin Photoreduction," *Molekul,* vol. 12, pp. 61-69, 2017.

[11] Y. Feng, Y. Ouyang and D. Liao, "Synthesis, Crystal Structure and Magnetic Properties of a Mn(III)Schiff Base Complex with One Dimensional Chain Structure Based on Hydrogen Bonds: [Mn(salpn)(CH_3OH)(4,4'bipy)](BPh_4)," *Acta Scientiarum Naturalium Universitatis Nankaiensis,* vol. 41, pp. 66-71, 2008.

[12] M. Okuhata and T. Mochida, "Thermal Properties and Crystal Structures of Manganese(III)-salen Complexes with The Tf_2N Anion [Tf_2N = bis(trifluoromethanesulfonyl)amide)]," *Polyhedron,* vol. 43, p. 153–158, 2012.

[13] S. Grabner, P. Bukovec and N. Lah, "Two New Mononuclear Manganese(III) Salen Complexes," *Acta Chimica Slovenica,* vol. 62, pp. 255-260, 2015.

[14] M. Sutradhar, L. M. Carrella and E. Rentschler, "Mononuclear Mn(III) and Dinuclear Mn(III, III) Schiff Base Complexes: Influence of π–π Stacking on Magnetic Properties," *Polyhedron,* vol. 38, pp. 297-303, 2012.

[15] Z. Lü, M. Yuan, F. Pan, S. Gao, D. Zhang and D. Zhu, "Syntheses, Crystal Structures, and Magnetic Characterization of Five New Dimeric Manganese(III) Tetradentate Schiff Base Complexes Exhibiting Single-Molecule-Magnet Behavior," *Inorganic Chemistry,* vol. 45, pp. 3538-3548, 2006.

[16] Y. Kani, S. Ohba, S. Ito and Y. Nishida, "Four Copper(II) Complexes with Potentially Tetradentate Tripodal Ligands," *Acta Crystallographica Section C,* vol. 56, pp. 233-235, 2000.

[17] A. Haikarainen, J. Sibila, P. Pietikainen, A. Pajunen and I. Mutikainen, "Synthesis and Characterization of Bulky Salen-Type Complexes of Co, Cu, Fe, Mn and Ni with Amphiphilic Solubility Properties," *Journal of the Chemical Society, Dalton Transactions,* vol. 5, pp. 991-993, 2001.

[18] L. J. Boucher and M. O. Farrell, "Manganese Schiff's Base Complexes—I: Synthesis and Spectroscopy of Some Anion Complexes of (4-sec-Butylsalicyaldehydeethylenediiminato) Manganese(III)," *Journal of Inorganic and Nuclear Chemistry,* vol. 35, pp. 3731-3738, 1973.

[19] V. A. Kostyuk, A. I. Potapovich, T. V. Kostyuk and M. G. Cherian, "Metal Complexes of Dietary Flavonoids: Evaluation of Radical Scavenger Properties and Protective Activity Against Oxidative Stress In Vivo," *Cellular and Molecular BiologyTM,* vol. 53, pp. 61-68, 2007.

[20] G. M. Sheldrick, "SHELXT-2014," *Acta Crystallography,* no. A71, pp. 3-8, 2015.

[21] G. M. Sheldrick, "SHELXL-2016," *Acta Crystallography,* no. C71, pp. 3-8, 2015.

[22] DIAMOND 3, K. Brandenburg, *Crystal Impact GbR,* Bonn, Germany.

Synthesis	**Crystal Structure of : [{Mn(salen)(ClO_4)}$_2$(μ-4,4'-bpy)] (1)**	**Research Paper**
Deawati, Y., Onggo, D., Muyani, I., Hastiawan, I., Kurnia, D., Lonnecke, P., Schmorl, S., Kersting, B., Hey-Hawkins, E.	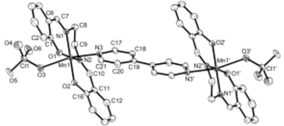	
	Coordination polymer along (010) of {[Mn(salen)(μ-4,4'-bpy)]PF_6}$_n$·1.5MeOH·0.5H_2O (2)	
	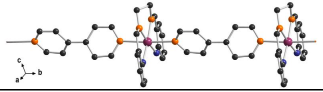	

Synthesis, Crystal Structures, and Superoxide Dismutase Activity of Two New Multinuclear Manganese(III)-Salen-4,4'-Bipyridine Complexes

Yusi Deawati*[1], Djulia Onggo[1], Irma Mulyani[1], Iwan Hastiawan[2], Dikdik Kurnia[3], Peter Lönnecke[4], Sara Schmorl[4], Berthold Kersting[4], Evamarie Hey-Hawkins[4]

HIGHLIGHTS:

- So far, no multinuclear manganese(III)-salen reported as SOD mimics.

- Here, we report the synthesis and characterization of manganese(III)-salen multinuclear complexes containing 4,4'-bpy bridging ligand and ClO_4^- axial ligand or PF_6^- counter anion. This study is neded to investigate the effect of multinuclear structural to SOD activity.

- Two new multinuclear manganese(III)-salen complexes containing 4,4'-bipyridine bridging ligand and ClO_4^- axial ligand or PF_6^- counter anion, namely dimeric $[\{Mn(salen)(ClO_4)\}_2(\mu\text{-}4,4'\text{-}bpy)]$ (**1**), and polymeric $\{[Mn(salen)(\mu\text{-}4,4'\text{-}bpy)]PF_6\}_n$ (**2**), were prepared and structurally characterized. Their SOD mimic activity was determined and indicates that structural features affect SOD activity.